Altitudinal Trends on Seasonal and Geographic Contrail Persistent Regions Over CONUS

Jimin Park[1]
NASA Ames Research Center, Moffett Field, California, 94035, USA

Addressing contrail formation and avoidance will play a large part in the aviation sector's fight against climate change. Most contrail research has focused on looking at contrail trends below 40,000 ft, the altitude range typically flown by commercial aircraft. Many next generation aircraft are designed to fly higher, such as the Sustainable Flight Demonstrator (SFD)'s Transonic Truss-Braced Wing (TTBW)'s cruise altitude 43,000 ft. This is significantly higher than that of its replacement, the Boeing 737-Max (B737). The Schmidt-Appleman criterion is used with weather data from the National Oceanic and Atmospheric Administration to take a closer look at contrails' seasonal and geographical trends over the Continental United States (CONUS). It is found that for the lower altitude range between 30,000 and 35,000 ft, as altitude increases there are more contrail persistent regions (CPR). However, the trend reverses after 40,000 ft to 50,000 ft, and the area of CPR decreases as altitude increases. Contrail seasonal and geographical dependence also depends on altitude, with lower altitudes having more CPR in the winter and spring in the north and northwest. Higher altitudes have more CPR during the summer and fall in the south. However, B737 common flight paths dominate in the south, making the southern section of the CONUS have more flights through CPR.

I. Nomenclature

c_p	=	specific heat capacity of air
e^{liq}_{sat}	=	water vapor pressure ratio
EI_{H2O}	=	emission index of water
G	=	slope of isobaric mixing line
p	=	ambient air pressure
Q	=	combustion heat of fuel
RH_i	=	relative humidity with respect to ice
RH_w	=	relative humidity with respect to water
r_{contr}	=	critical relative humidity
T	=	ambient temperature
T_{contr}	=	threshold temperature
ε	=	molecular mass ratio of water and air
η	=	propulsive efficiency of aircraft engine

II. Introduction

There has been a rising level of interest in contrails and their impact on global climate change. Contrails are line shaped clouds that form behind aircraft when flown at certain atmospheric conditions [1]. Water vapor emitted from aircraft cool and condense onto particulate matter in the local atmosphere. The particulate matter may be from the same aircraft or already present in the atmosphere. Most contrails do not have a long time span, but in ice

[1] Aerospace Engineer, Experimental Aero-Physics Branch.

supersaturated regions (ISSR), persistent contrails may last up to 18 hours [2] and eventually merge with other clouds already present.

Contrails have a significant impact on global radiative forcing. In 2018, contrail cirrus clouds contributed 111 (high and low estimates of 33 and 189) mWm^{-2} to global radiative forcing, as compared to 34 (high and low estimates of 31 and 38) mWm^{-2} from CO_2 with a 95% confidence interval [3]. However, the warming effects from contrails are more temporal than those from CO_2 and are contained to localized areas. Regional atmosphere, seasons, and time of day all have a large impact on contrail formation and consequence. Thus, in addition to aircraft technology development, air traffic rerouting is an area that is being widely considered as a potential solution for contrail prevention. One study from Teoh et al. [4] looks at diverting less than 2% of the fleet over the Japanese airspace above or below contrail persistent regions (CPR) to reduce contrail energy forcing by 59% for a 0.014% increase in fuel consumption.

NASA's Electrified Powertrain Flight Demonstrator (EPFD) [5] and Sustainable Flight Demonstrator (SFD) [6] projects aim to demonstrate the implementation of two distinct sustainable aircraft concepts with a predicted entry into service of 2035. In particular, the SFD Transonic Truss-Braced Wing (TTBW) represents the next generation narrow body single aisle aircraft and targets to replace the currently flying Boeing 737-Max (B737). The B737, like many commercial aircraft, generally flies at altitudes of 30,000 to 40,000 ft; a significantly lower altitude than the TTBW's target cruise altitude of 43,000 ft. Thus, making the same assumptions for the TTBW as those from current commercial aircraft to conduct contrail avoidance would be ill-advised, seeing that the TTBW will be flying under very different atmospheric conditions.

Historically, contrail trends have been most often looked at over Europe and at the lower altitudes flown by most currently flying commercial aircraft. Dischl et al. [7] studied at the seasonal variation in persistent contrails above Europe at around 30,000 to 39,000 ft. Minnis et al. [8] investigated contrails forming over select locations in the Continental United States (CONUS) Since the work was conducted using observed contrails, the data is sparse and only shows contrails that were formed due to the aircraft from that current generation. Contrail patterns at higher altitudes, such as those the TTBW will fly at, and over the entirety CONUS are not well understood.

In this paper, contrail patterns over CONUS have been analyzed to identify any geographical or seasonal trends at altitudes between 30,000 and 50,000 feet. By looking at this wider region, we hope to identify the contrail hotspots for next generation aircraft and prevent air traffic over-management for future implementations of contrail avoidance rerouting.

III. Methods and Data

A. Schmidt-Appleman Criteria

The main methodology used in this paper to assess CPR is the Schmidt-Appleman criterion along with ISSR for contrail persistence [9]. The Schmidt-Appleman criterion is a widely used model to find the threshold atmospheric conditions that would allow for contrail formation. If the atmosphere an aircraft flies through has a low enough temperature with high humidity, a contrail is formed due to liquid saturation [10].

The threshold temperature is given by Eq. (1) and the slope of the isobaric mixing line is given in Eq. (2)

$$T < T_{contr} = -46.46 + 9.43\ln(G - 0.053) + 0.72ln^2(G - 0.053) \tag{1}$$

$$G = \frac{p\, c_p}{\varepsilon} \frac{EI_{H2O}}{(1-\eta)\, Q} \tag{2}$$

The relative humidity with respect to water (RH_w) must be greater than the critical relative humidity (r_{contr}), which can be found using Eq. (3). The water vapor pressure ratio can be found using Eq. (4). The condition that RH_w must be lower than 100% is added to the Schmidt-Appleman criterion in this paper since RH_w at 100% indicates a cloud is already present.

$$1 > RH_w > r_{contr} = \frac{G(T - T_{contr}) + e_{sat}^{liq}(T_{contr})}{e_{sat}^{liq}(T)} \tag{3}$$

$$e_{sat}^{liq}(T) = 6.0612\exp\left(\frac{18.102T}{249.52+T}\right) \tag{4}$$

Most contrails don't last longer than 10 minutes and have a small climate impact [1]. However, persistent contrails formed in ISSR last for hours and contribute more radiative forcing. ISSRs occur when the relative humidity to ice (RH_i) is greater than 100%. RH_i can be found using Eq. (5).

$$RH_i = RH_w \frac{6.0612\exp\left(^{18.102T}/_{249.15+T}\right)}{6.1162\exp\left(^{22.577T}/_{273.38+T}\right)} \tag{5}$$

For the purposes of this paper, only CPR are considered. The Schmidt-Appleman criterion in ISSR is evaluated at each spatial datapoint at specified time intervals in 2018. Constant parameters used are listed in Table 1.

Table 1: Parameters held constant to calculate the Schmidt-Appleman criterion

Parameter	Value
EI_{H2O}	1.25
c_p	1004 J Kg^{-1} K^{-1}
η	0.3
Q	42000000 J Kg^{-1}
ε	0.622

B. Meteorological Data

The National Oceanic and Atmospheric Administration (NOAA) publishes hourly atmospheric data made from a numerical forecast model for public use. For this paper, temperature and RH_w Rapid Refresh (RR) data from 2018 at altitudes 30,000, 35,000, 40,000, 45,000, and 50,000 ft are used. RR has a horizontal spatial resolution of 13 km, vertical isobaric pressure level resolution of 25 hPA, and one hour temporal resolution. NOAA covers the CONUS region with longitude and latitude data of -139.9◦ to -57.3◦ and 16.2◦ to 59.0◦ respectively. Several days and hours are skipped during analysis due to missing weather data and are listed in Table 2.

Table 2: Dates and Times of Missing RR Data

Date	Time (UTC)
01/13/2018	02:00 to 23:00
01/14/2018	00:00 to 20:00
01/18/2018	10:00 to 20:00
11/03/2018	4:00

IV. Results

CPR over CONUS are calculated using the Schmidt-Appleman criterion with NOAA RR data as described in Section III. To view temporal trends throughout the year, total CPR area is summed from data points taken every 3 hours for every other day. Datapoints are filtered through a Savitzky-Golay filter for trend clarity, and the plotted results are shown in Fig. 1.

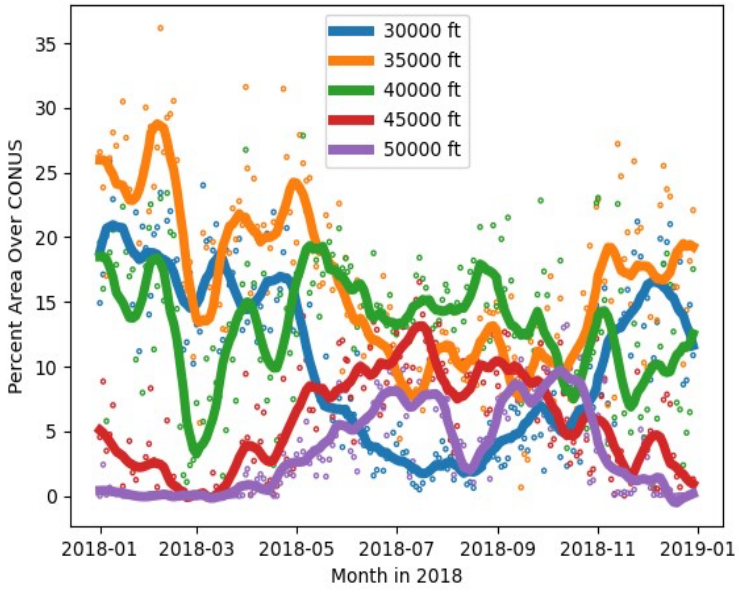

Fig. 1: Percent of CONUS covered by CPR through 2018, by altitude

At lower altitudes, particularly at 30,000 and 35,000 ft, the trends for CPR follow the observation that contrails decrease over CONUS in the summer months [8]. Europe seems to follow this trend as well [7]. However, as the altitude increases, the trend flips and the winter and spring months have a very small amount of CPR while the summer months have a significant increase. It is noticeable that total CPR area over the entire year at higher altitudes (45,000 and 50,000 ft) is less than that of the lower altitudes (30,000 and 35,000 ft). Only during the summer do the higher altitudes have a larger area of CPR. This is mainly caused by the colder temperatures at higher altitudes. Lower altitude regions usually do not get cold enough to create contrails during the summer and thus CPR drops off. At higher altitudes, the temperature remains cold enough for contrail formation, and persistent contrail formation becomes mainly restricted by a low RH_i unsuitable for ice super-saturation.

The effects of seasonality on contrail geographic location and day and night cycles are observed as well. The average sunrise and sunset times from the east and west coasts are taken to define the day and night times. Dates and times used are shown in Table 3.

Table 3: Date and Day/Night Time for Each Season

Season	Date	Day Time	Night Time
Spring	03/21/18 to 06/21/18	05:30 to 19:30	19:30 to 05:30
Summer	06/22/18 to 09/22/18	05:30 to 19:30	19:30 to 05:30
Autumn	09/23/18 to 12/21/18	06:30 to 18:30	18:30 to 06:30
Winter	01/01/2018 to 03/20/18, 12/22/18 to 12/31/18	06:30 to 18:30	18:30 to 06:30

The effect of day and night and of increasing propulsive efficiency on CPR area trends are analyzed in Fig. 2 and 3. While a standard 0.3 propulsive efficiency for gas turbine driven engines is used for all analysis, the TTBW has a predicted propulsive efficiency of around 0.376. However, no new noticeable seasonal or altitudinal trends are observed, as shown.

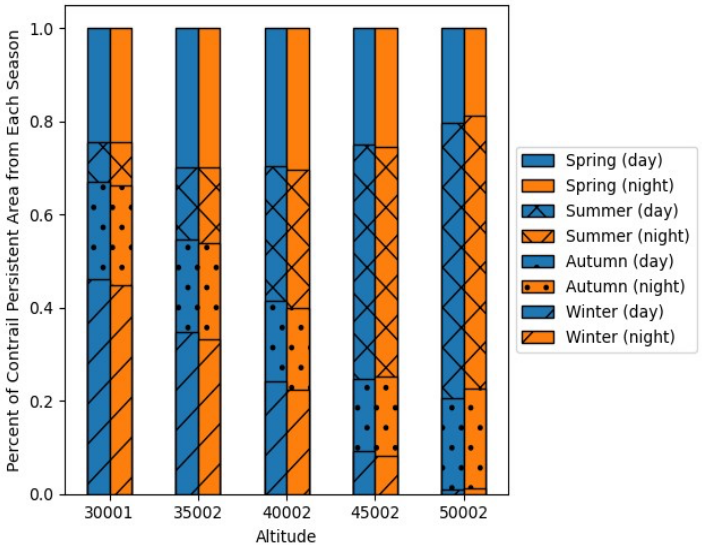

Figure 2: Comparison of percent of CPR area over CONUS for each season for day and night

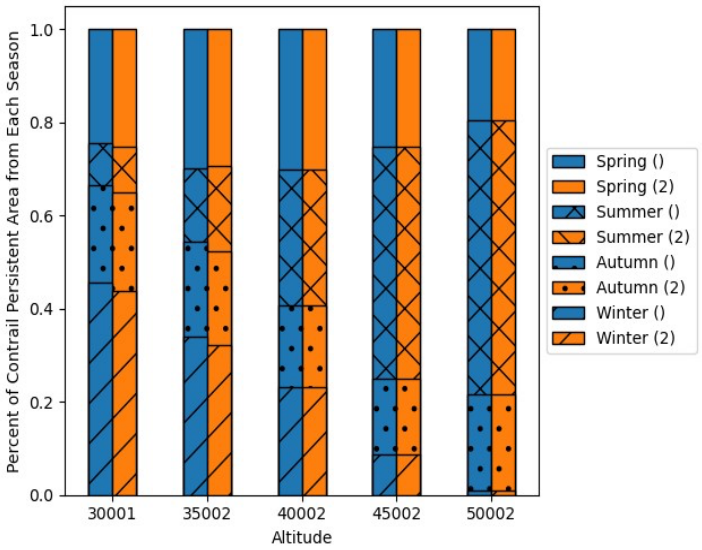

Figure 3: Comparison of percent of CPR area over CONUS for each season for propulsive efficiency of 0.3 and 0.376

CPR over CONUS in 2018 at 30,000 to 50,000 ft are shown in Fig. 4 through 7. At the lower altitudes there are more CPR overall, with a higher concentration in the northern section of CONUS. There is a particularly high concentration in the northwest section during spring and winter. The formation of these regions is driven by the temperature threshold, where only northern regions are cold enough to sustain persistent contrails. The RH_w is generally lower than the r_{contr} in the south, also contributing to fewer contrails in southern lower altitudes. However, as the altitude increases, the CPR become sparse and shift towards the south, with the summer and autumn seasons having more CPR covering CONUS territory due to a constraint in RH_i.

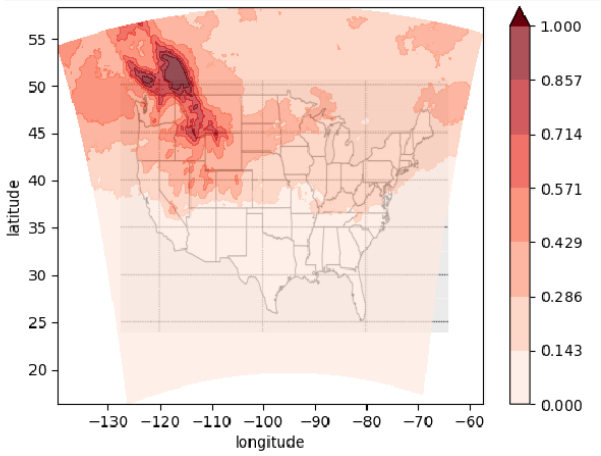

(a) 2018 Spring, FL 300

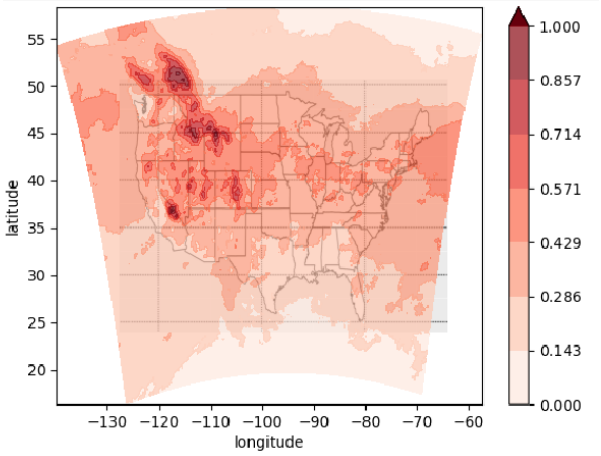

(b) 2018 Spring, FL 350

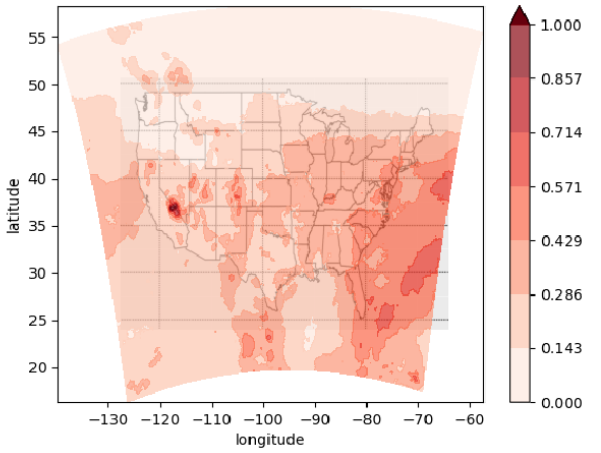

(c) 2018 Spring, FL 400

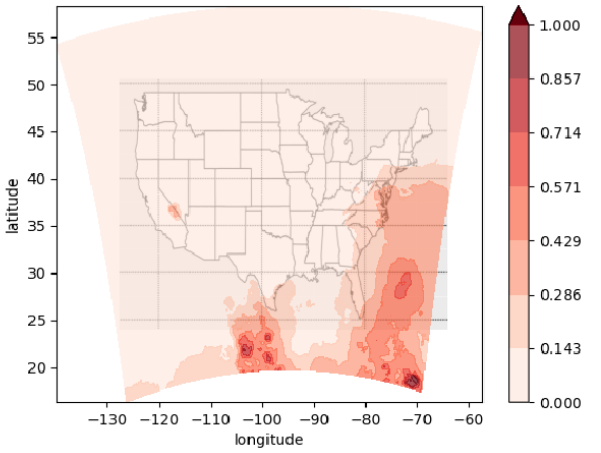

(d) 2018 Spring, FL 450

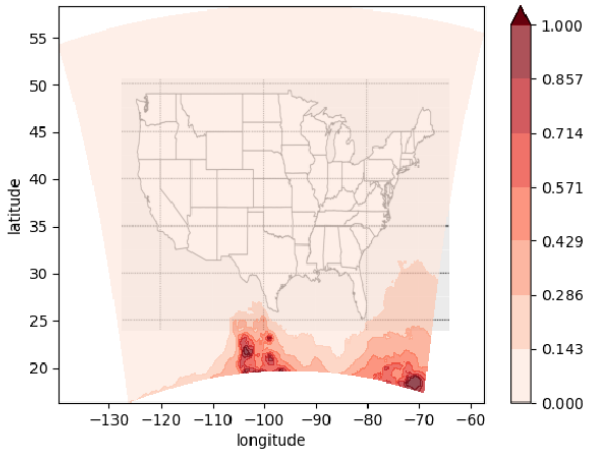

(e) 2018 Spring, FL 500

Figure 4: CPR over CONUS at flight levels 300 to 500 during spring 2018. Darker regions indicate more CPR formation over the season. Coloring is normalized over all seasons and altitudes in 2018.

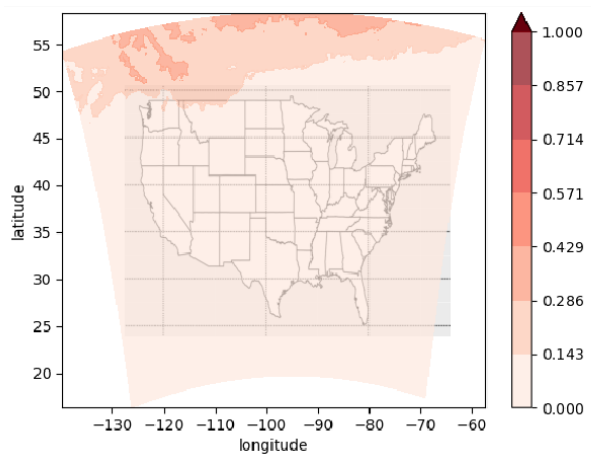

(a) 2018 Summer, FL 300

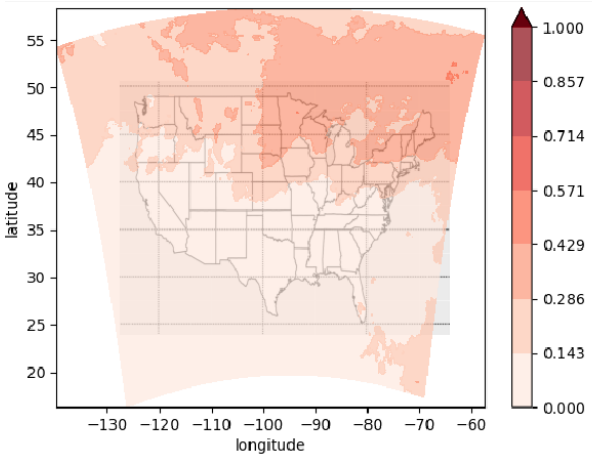

(b) 2018 Summer, FL 350

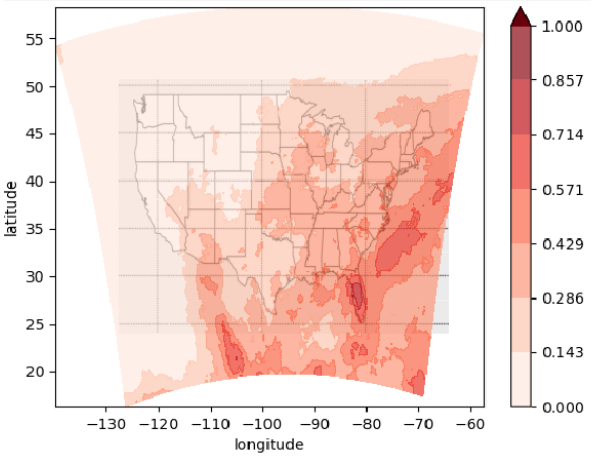

(c) 2018 Summer, FL 400

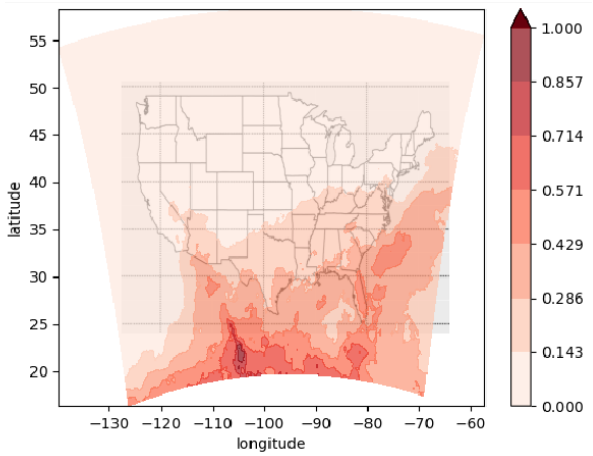

(d) 2018 Summer, FL 450

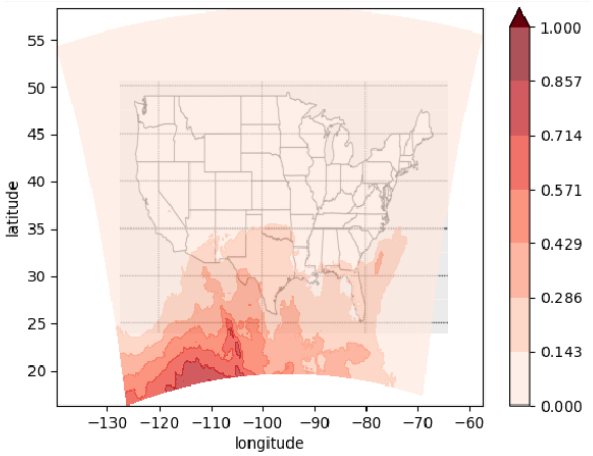

(e) 2018 Summer, FL 500

Figure 5: CPR over CONUS at flight levels 300 to 500 during summer 2018. Darker regions indicate more CPR formation over the season. Coloring is normalized over all seasons and altitudes in 2018.

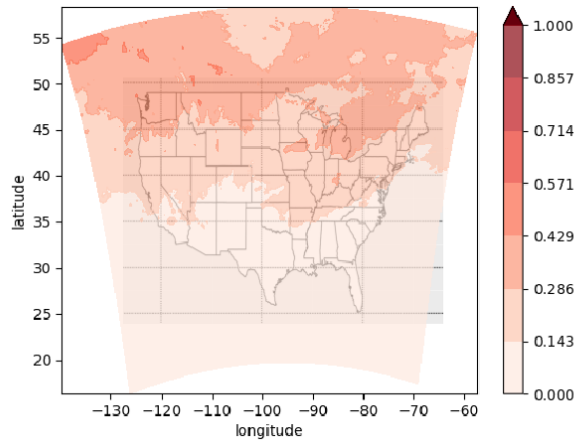

(a) 2018 Autumn, FL 300

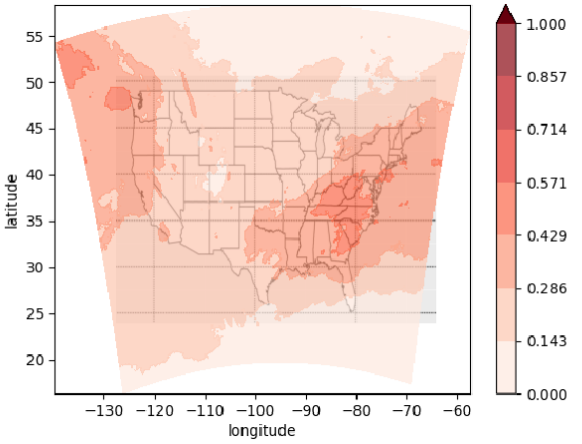

(b) 2018 Autumn, FL 350

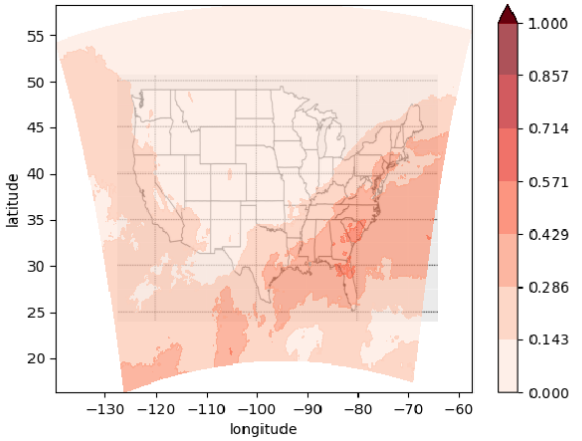

(c) 2018 Autumn, FL 400

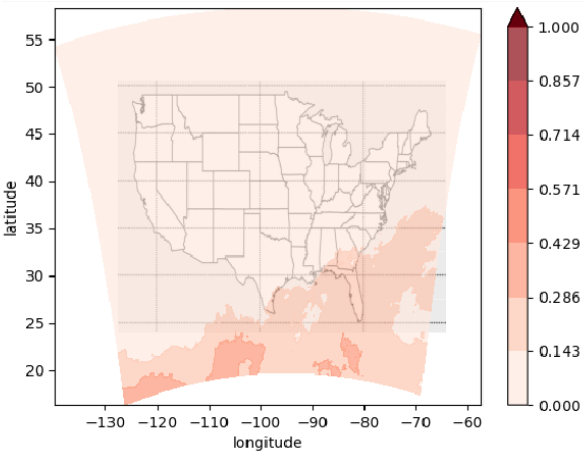

(d) 2018 Autumn, FL 450

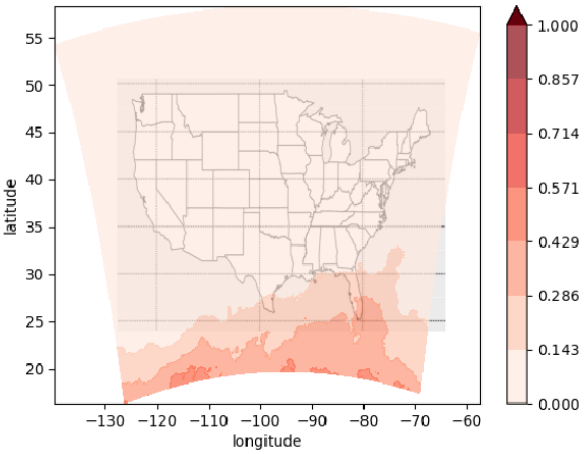

(e) 2018 Autumn, FL 500

Figure 6: CPR over CONUS at flight levels 300 to 500 during autumn 2018. Darker regions indicate more CPR formation over the season. Coloring is normalized over all seasons and altitudes in 2018.

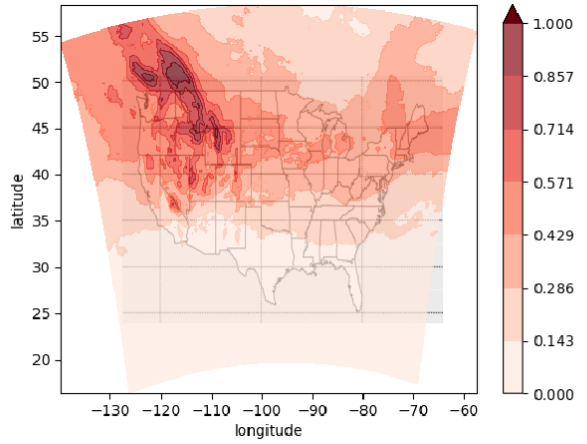

(a) 2018 Winter, FL 300

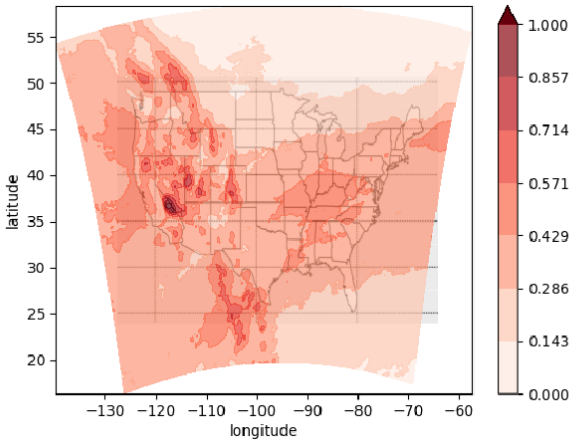

(b) 2018 Winter, FL 350

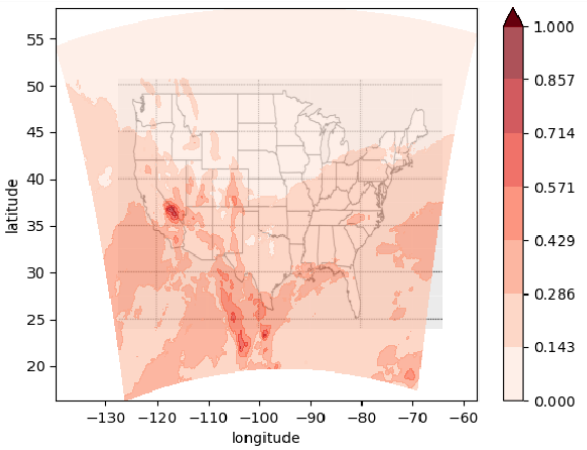

(c) 2018 Winter, FL 400

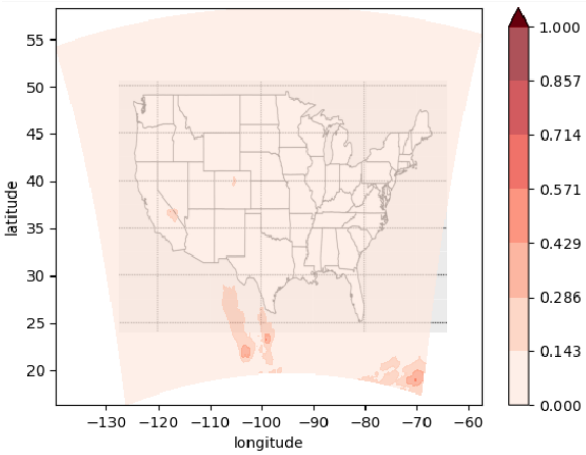

(d) 2018 Winter, FL 450

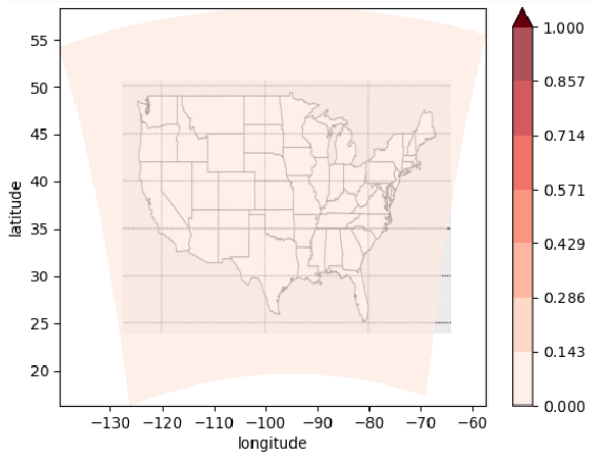

(e) 2018 Winter, FL 500

Figure 7: CPR over CONUS at flight levels 300 to 500 during winter 2018. Darker regions indicate more CPR formation over the season. Coloring is normalized over all seasons and altitudes in 2018.

To take a closer look at how the CPR may interact with aircraft flight paths, trajectories of B737 flying over CONUS in 2018 are overlaid on the CPR contours. Flight origin and destinations are taken from Bureau of Transportation Statistics (BTS), and the flight path is assumed to be a great circle path between the two. A constant flight altitude of 35,000 or 43,000 ft and a constant ground speed are also assumed. The two altitudes represent current and next generation aircraft cruise altitudes. An example trajectory of a random month in 2018 is shown in Fig 8. From visual inspection, each month had a similar distribution of flight paths over CONUS. To match the atmospheric data to the flight trajectory waypoints, the trajectory is split into hour increments. The closest RR coordinate is matched to the aircraft's coordinate at each hour, and possible contrail creation is determined. Possible contrail creation along the flight trajectories each month are shown in Fig. 9 and 10.

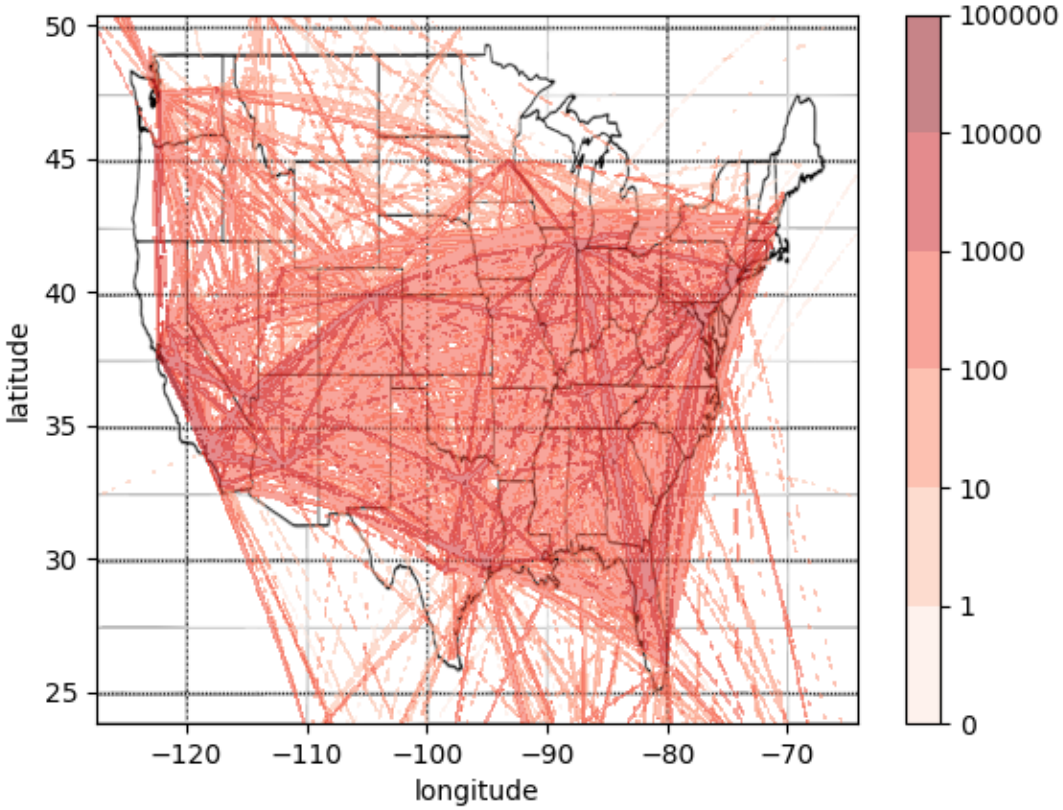

Figure 8: Trajectories of B737 flying over CONUS according to BTS data during a random month in 2018. Darker regions indicate more B737 trajectories flew over that area. Coloring of trajectories is on a log scale.

The overlaid trajectories with CPR reflect many of the trends found earlier. Higher altitude trajectories fly through fewer CPR than lower trajectories. Though it is difficult to see on the log scale, the lower trajectories fly through fewer CPR in the summer months. More noticeably, the higher altitude trajectories fly through more CPR in the summer months.

The overlaid trajectories reveal geographic trends that are not apparent in Fig. 2 through 5. Although atmospheric conditions may be hospitable for persistent contrails to form at lower altitudes, not enough aircraft fly through the northern parts of CONUS to show significant possible contrail creation. Instead, most of the possible contrail creation seem to form around the rest of CONUS and particularly on the coasts. Higher altitudes show that possible contrail creation would focus around the east and south of CONUS during the summer months, and just south of CONUS throughout the rest of the year. However, it is important to note that only B737 trajectories at a constant flight altitude are shown. Other aircraft and changing flight altitudes during climb or descent may heavily influence the trends shown.

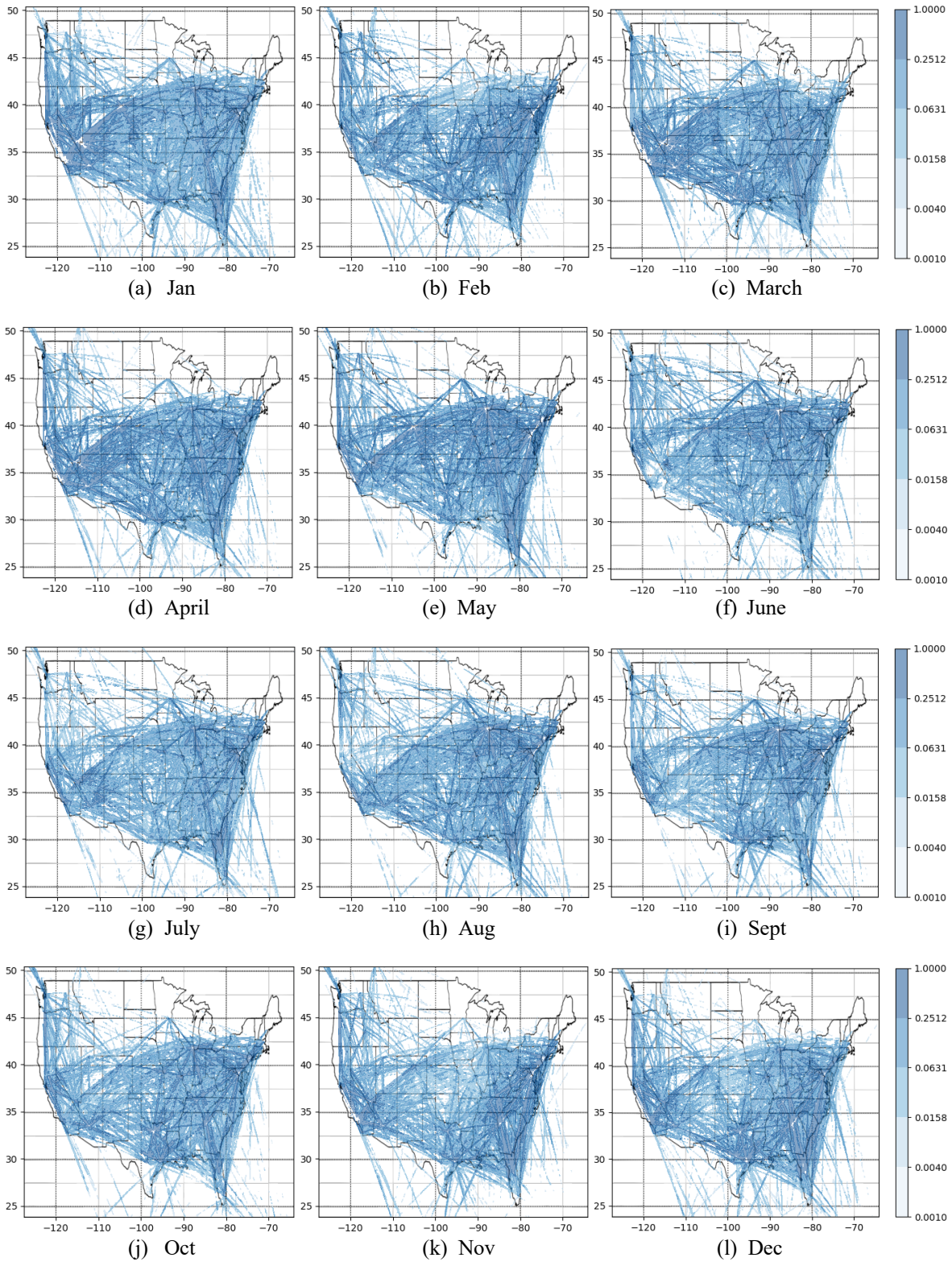

Figure 9: Trajectories of B737 flying over CONUS at 35,000 ft overlaid on CPR in 2018. Darker regions indicate more trajectories flew over that area when CPR were present. Coloring is normalized and on a log scale.

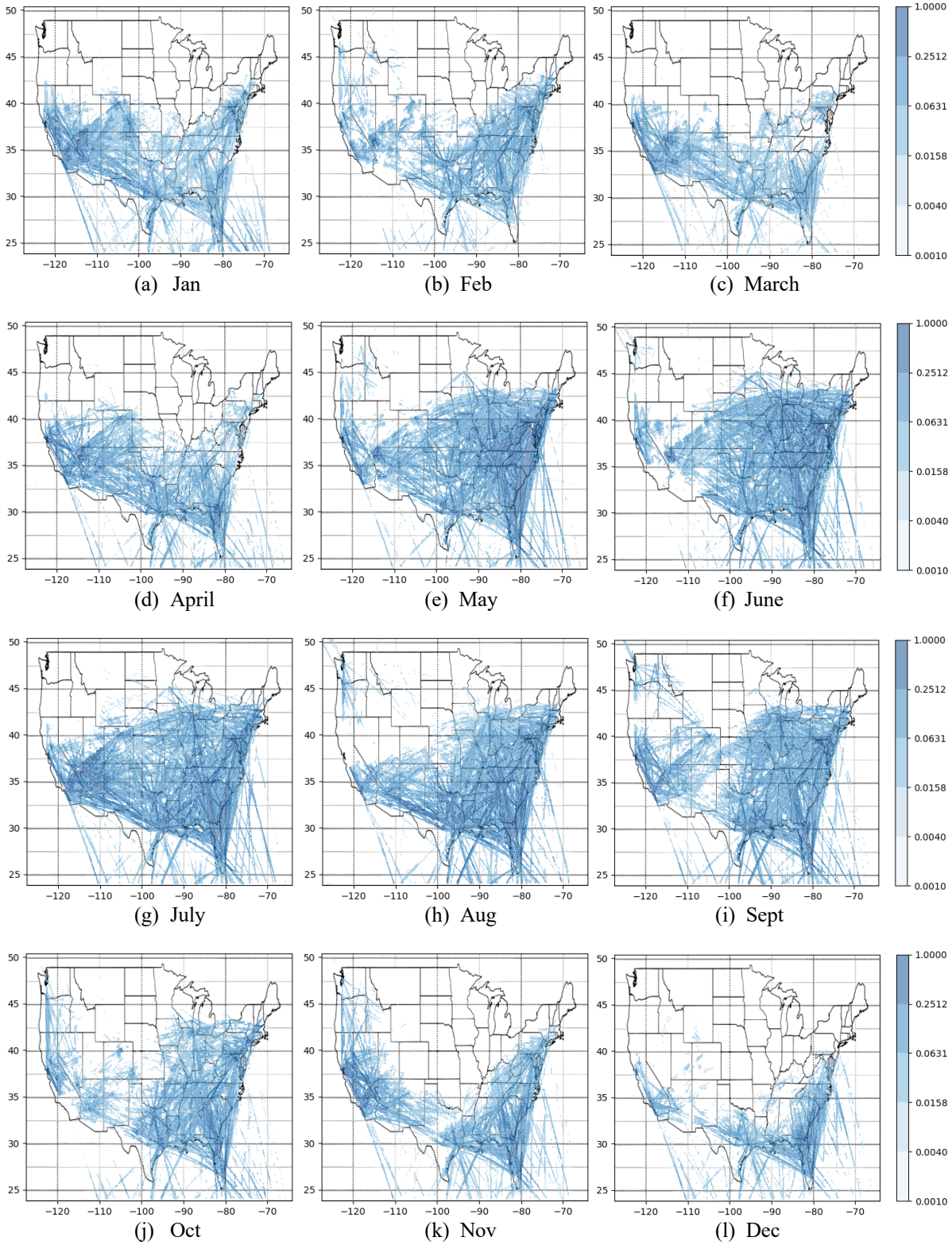

Figure 10: Trajectories of B737 flying over CONUS at 43,000 ft overlaid on CPR in 2018. Darker regions indicate more trajectories flew over that area when CPR were present. Coloring is normalized and on a log scale.

V. Conclusion

This paper looks at the seasonal and geographical trends of contrail persistent regions 30,000 to 50,000 ft above CONUS. NOAA rapid refresh data is used with the Schmidt-Appleman criterion and ice super-saturation to determine contrail persistence.

Looking at the trends in CPR over CONUS, more CPR are created as altitude increases, peaking in the spring and winter months. The trend flips after 40,000 feet and the formation of CPR decreases as altitude increases further. The spring and winter months have fewer CPR than the summer and autumn months at these higher altitudes. These trends are determined by constraints in humidity and temperature and seem to focus on different geographical locations above CONUS. The lower altitudes have more CPR overall but particularly in the north and northwest, while the higher altitudes have more in the south. However, overlaying B737 flight paths at low and high altitudes on the CPR contours show that for both altitudes not enough flights fly in northern CONUS, and the southern and coastal regions dominate in terms over possible contrail creation.

The B737 aircraft typically cruises at around 30,000 to 40,000 ft. At this altitude range, a significant portion of CONUS is covered in CPR. The TTBW's preference towards higher cruise altitudes allows it to avoid more CPR over the entire year than the B737 without any additional aircraft redirection. For further contrail avoidance, air traffic control within CONUS would only need to focus on redirecting the TTBW around the summer months in the southern regions.

The Schmidt-Appleman criterion and the results found are dependent on the reliability of the weather data available. While temperature forecasts are fairly reliable, relative humidity is much more difficult to predict [11, 12]. It is possible that the discovered trends fall apart when a large uncertainty in weather data is introduced. It is also possible that the results only appear in 2018, and that CPR in other years follow different patterns. Further analysis needs to be done on the sensitivity of the results to weather prediction and if the trends are repeatable for other years.

To take a closer look at the difference in contrail generation between current and next generation aircraft, an ongoing study replaces B737 flights from the past with hypothetical higher altitude aircraft using the NAS Digital Twin (NDT) [13]. NDT is a physics-based environment that simulates past, current, and future airspace operations. NDT uses the Schmidt-Appleman criterion or postprocesses its results using a python-based package of the Contrail Cirrus Prediction Tool (CoCip) [14, 15].

References

[1] Kärcher, B. (2018) 'Formation and radiative forcing of contrail cirrus', Nature Communications, 9. doi:10.1038/s41467-018-04068-0.

[2] Haywood, J. M., Allan, R. P., Bornemann, J., Forster, P. M., Francis, P. N., Milton, S., Rädel, G., Rap, A., Shine, K. P., and Thorpe, R. (2009) 'A case study of the radiative forcing of persistent contrails evolving into contrail-induced cirrus', Journal of Geophysical Research: Atmospheres, 114(D24). doi:10.1029/2009jd012650.

[3] Lee, D.S. et al. (2021) 'The contribution of global aviation to anthropogenic climate forcing for 2000 to 2018', Atmospheric Environment, 244. doi:10.1016/j.atmosenv.2020.117834.

[4] Teoh, R. Schumann, U., Majumdar, A., and Stettler, M. E. J. (2020) 'Mitigating the Climate Forcing of Aircraft Contrails by Small-Scale Diversions and Technology Adoption', Environmental Science & Technology, 54(5), pp. 2941–2950. doi:10.1021/acs.est.9b05608.

[5] Gipson, L. (2024, September 26). *About Electrified Powertrain Flight Demonstration Project*. NASA. https://www.nasa.gov/directorates/armd/integrated-aviation-systems-program/armd-iasp-epfd/about-electrified-powertrain-flight-demonstration-project/

[6] Gipson, L. (2023, January 18). *About Sustainable Flight Demonstrator Project*. NASA. https://www.nasa.gov/directorates/armd/integrated-aviation-systems-program/armd-iasp-sfd/about-sustainable-flight-demonstrator-project/

[7] Dischl, R., Kaufmann, S. and Voigt, C. (2022) 'Regional and Seasonal Dependence of the Potential Contrail Cover and the Potential Contrail Cirrus Cover over Europe', Aerospace, 9(9), p. 485. doi:10.3390/aerospace9090485.

[8] Minnis, P., Ayers, J. K., Nordeen, M. L., and Weaver, S. P. (2003) 'Contrail frequency over the United States from Surface Observations', Journal of Climate, 16(21), pp. 3447–3462. doi:10.1175/1520-0442(2003)016<3447:CFOTUS>2.0.CO;2.

[9] Appleman, H. (1953) 'The Formation of Exhaust Condensation Trails by Jet Aircraft', Bulletin of the American Meteorological Society, 34(1), pp. 14–20. doi:10.1175/1520-0477-34.1.14.

[10] Chen, N. Y., Sridhar, B. and Ng, H. K. (2012) 'Tradeoff between contrail reduction and emissions in United States National Airspace', Journal of Aircraft, 49(5), pp. 1367–1375. doi:10.2514/1.c031680.

[11] Gierens, K., Matthes, S. and Rohs, S. (2020) 'How well can persistent contrails be predicted?', Aerospace, 7(12), p. 169. doi:10.3390/aerospace7120169.

[12] Weygandt, Steve. (2021) ‘A History of Operational NWP Improvements’, Presentation [Online]. Available: https://gsl.noaa.gov/science_review_2021/presentations/EarthSystemPrediction-AcrossScales.pdf
[13] Lauderdale, T., Thipphavong, D. and Park, J. (2023) ‘Exploratory Contrail Studies: Transonic Truss-Braced Wing (TTBW) Contrail Assessment & National Airspace System (NAS) Impacts from Contrail Avoidance’, Presentation [Online]. Available: https://ntrs.nasa.gov/citations/20230015962.
[14] Breakthrough Energy Foundation. (2025, May 15). p*ycontrails*. Breakthrough Energy. https://py.contrails.org/
[15] Schumann, U. (2012) ‘A contrail cirrus prediction model’, Geoscientific Model Development, 5(3). doi:10.5194/gmd-5-543-2012.